1
Introduction

The history of electric power generation dates back to 1800 when Alessandro Volta used chemical reaction in an electrolytic cell to generate electricity, however the method was costly. Generation of a power on a large scale was not feasible, until in 1831 Michael Faraday devised a rotary machine to generate the electricity. It took about half a century for the technology to become available at the commercial stage. The first steam powered electricity generation was setup at Holborn Viaduct in London, in 1882 by Thomas Edison. The electricity was used for street lightening, but soon it was provided for local consumers. The electricity generated was DC in nature. The voltage level of electricity generated cannot be changed easily. Due to this, the power was locally generated and consumed. Further, the size of cables used for power delivery cannot be reduced as the voltage levels have to be increased to do so. This is considered to be a drawback in the Edison's concept of power generation and distribution. On the other hand, mid 1880s witnessed an introduction of the alternating current (AC) systems in US and Europe. The main advantage of using an AC system was the availability of transformers. The AC transformers were used to step up or step down the voltage. This facilitated reduction of the power conductor size and distribution losses by stepping up of the voltage. This made the power transmission more economical compared to its DC counterpart. The technical and economical advantages of an AC system is more to overwhelm the DC power generation system. Industrialists such as George Westinghouse, Galileo Ferraris, Carl Wilhelm Siemens, Nikola Tesla advocated the advantages of AC over the DC system. This led to a rapid installation of the AC power generation and distribution system throughout the world and is the foundation for the modern AC grid system.

The AC power generation facilitated the power to be generated at remote locations, and transmit it towards the consumption areas. The generation stations are connected through a grid network to ensure the intermittent power supply. The power generation stations use non-renewable sources such as coal, natural gas, and petroleum products. The coal and oil-based power plants have efficiency in the range of 30-40%. The gas-powered plants have an efficiency of about 50-60%. The power hence generated is to be transmitted over a long distance. In India, the power loss in transmission and distribution is about 15-20% of generation. Hence, a huge chunk of power is lost, which further lowers the overall efficiency. Further, continuously depleting fossil fuels and ever-growing demand for uninterrupted power poses a challenge for the traditional power generation and distribution system. The power generation methodologies in these power plants lead to emission of pollutants such as NO_x, CO_2, CO, SO_x organic gases. These pollutants are known to be harmful to the environment and its inhabitants. In order to reduce greenhouse gas emissions into the atmosphere, the Kyoto protocol regulations have been signed among the member developing nations. The Kyoto Protocol was adopted on 11^{th} December 1997 and came into force on 16^{th} February 2005. To achieve the aim of carbon emission reduction, a paradigm shift in power generation is being observed from non-renewable sources to renewable sources such as photo-voltaic panels, wind turbines, hydro-power, bio-mass power, etc. Recent years have observed a continuous increase in the number of projects and research work on formulation of an efficient and reliable microgrid, for supporting the traditional AC grid system. The power generation units based on renewable sources can also be interconnected to form a local micro-grid or a nano-grid. The power is locally generated and consumed; hence, the long transmission is not

required. Unlike the traditional power generation system, the power from a renewable source is DC in nature as in photovoltaic cells, fuel cells, etc, which makes the interconnection easier. The power from sources like wind turbines can be converted to DC and then connected to the micro-grid, using AC-DC power electronic converter. Further, the loads such as LED lights, data centers, and energy storage batteries etc are inherently DC in nature.

The enhancement in power electronic technology has paved way for ease in power processing in AC-DC, or DC-AC conversions. Power electronics started with formulation of a mercury arc based rectifier which was developed in 1902 to perform AC-DC conversion. The solid state transistors were developed in 1948, and were easier to control compared to the mercury arc based valves. From 1950 onwards, high power semiconductor devices such as diodes, silicon controlled rectifier (SCR), etc were developed, which increased the range of applications of power electronic devices. The issue with the SCRs is that it requires a separate circuit for commutation. This paved way for necessity of high power devices which can be easily turned on or off. As a result of this, devices such as bipolar junction transistor (BJT) was developed in 1970. These are used to control low or medium power applications. The BJT have high switching losses and hence, there is a limit of frequency upto which it can be operated. This disadvantage of BJTs led to formulation of the metal oxide field effect transistors (MOSFETs) in 1978. The MOSFETS are used for low power high frequency applications. The BJTs and MOSFETs complement each other in terms of characteristics. On one hand, BJTs can regulate higher voltages and currents compared to MOSFETs, on the other hand, MOSFETs can operated at much higher frequencies due to much lesser switching losses. To fill the gap between the characteristics of both devices, there was a need of a device which can handle moderate or high voltages with higher switching frequency than the BJT but less than the MOSFETs. This led to the development of the insulated gate bipolar transistor (IGBTs) in 1983. Further, different high power, wide band-gap, high frequency devices such as SiC JFETs, SiC MOSFETs, Si CoolMOS, Cool Gallium Nitride (GaN) etc. have been developed so as to further improve the technology. These power electronic devices are used at the load end, to process the power as per the required voltage or frequency level. An inverter is used for DC-AC conversion, while a variable DC voltage can be obtained by using the buck, boost, or the buck-boost converter. Along with traditional DC-AC conversion techniques, various single stage inversion topologies have been proposed in the literature with the aim of reducing the component count and reducing the power loss in different stages. Topologies such as Z-source inverters (ZSI), quasi-Z-source inverters, Switched Inductor ZSI,Trans-ZSI, Inverse Watkins–Johnson topology, DC-link type SBIs have been proposed. These SSIs are used for nanogrid applications. Hence, a new paradigm of DC Microgrid and nanogrid is being setup so as to ensure power supply in remote locations. The DC Microgrids can further be integrated with the traditional grid system so as to improve the reliability of the power generation system.

The traditional generation and distribution system is designed to feed a sinusoidal voltage at a rated frequency to the load. In order to integrate these loads to the DC Microgrid, a DC-AC conversion is required. The inverter topologies like the VSIs and CSIs are used to feed the AC load. In order to achieve a higher voltage output at the ac terminals, two stage DC-DC-AC inverter topologies are used. It consists of an intermediate boost converter to step-up the DC voltage to some desired voltage level. In order to reduce the component count, the single stage inverters are also used, to achieve a higher output AC voltage. It incorporates the shoot through stage in which all the inverter switches are shorted. The single stage inverters have found applications ranging from- nanogrid, solar PV micro-inverters to electric vehicles etc. The VSIs, CSIs, or SSIs perform the DC-AC conversion. The output power of these topologies consist of a constant component and pulsating component of power. The constant component depends on the power factor of the load connected at the output terminals. The pulsating component oscillates at twice the inverter output supply frequency. The pulsating power at inverter output terminals leads to the reflection of the second-order harmonics at the DC end. This pulsating component leads to oscillations

in voltage and currents at the DC side. In DC-AC conversions, the second order harmonics are observed primarily in the source current, as the source voltage is nearly constant. In two stage DC-DC-AC conversion, the oscillations occur in terminal capacitor voltage. The ripple currents also propagates through the intermediate boost converter to the source. In SSIs, the DC-AC conversion takes place during the non-shoot through time interval. During this stage the power is delivered to the load. Hence, the second order ripples propagates through the impedance network of the SSIs to the source. In distributed power generation environment like the DC Microgrid, these SRCs get distributed among the network depending on the impedance of the interfacing converter, as seen from the DC bus. The converter which has low impedance has to bear more SRCs compared to the converters with high impedance. Further, the interconnecting line resistances also affect the SRC distribution. The SRCs propagate to the source in the absence of any SRC mitigation circuitry. Further, the DC Microgrid is also projected as a traditional grid support system. This means that the power generated by the microgrids is fed to the conventional grid system so as to ensure intermittent power supply to the load centers. Recently, there has been an increased research in the field of grid integration with the microgrid. The integration of microgrid with the conventional grid requires DC-AC conversion. This also causes the second order oscillations in the bus voltage and source currents.

1.1 MOTIVATION AND RESEARCH OBJECTIVES

The SRCs have various detrimental effects on the sources and battery storage. It leads to stress in the converter or inverter components. This may lead to failure of a component and hence, affects the reliability of the system. It leads to ripple torque in the wind turbines and leads to mechanical stress. The SRCs cause a rise in the temperature of the photo-voltaic panels. An increase in the temperature of PV panels leads to a reduction in the power generated. Further, the second-order voltage and current oscillations lead to varying maximum power point in PV panels. Hence, the maximum power may not be extracted from it. To mitigate the SRCs over sizing of the components is needed. In terms of batteries, the SRCs cause the depletion of electrodes, when drawn beyond a certain limit for a long time. It also causes a rise in battery temperature. The Lead Acid batteries is known to have more temperature rise when ripple currents are drawn from it compared to the Ni-Cd, or NaS batteries. The Lead acid batteries are less costly compared to the Ni-Cd or NaS batteries. To improve the life span of the sources, battery storages, and converter components, the SRCs must be mitigated or kept within the desired limits.

The SRCs can be regulated by active or passive methodology. In passive methodology, the size of passive components, i.e., inductance and capacitance, is increased so as to vary the impedance as seen from the DC bus. The capacitance size is increased to provide the oscillatory power during the DC-AC conversion. The frequency of second order ripples is usually low. This implies that a large size capacitor will be required to mitigate the SRCs. Usually the electrolytic capacitors are used instead of the aluminum, ceramic or film capacitors as the electrolytic capacitors are comparatively cheaper. However, the electrolytic capacitors are not reliable, and are known to have lesser life compared to the other components. The inductance of the converter can also be increased to reduce the SRC content. However, this leads to an increase in the weight of the system. Various active filters are also used with the aim of reducing the capacitance requirements. In distributed power generation, the installation of an active or passive filter will lead to an increase in the component count. This will increase the cost and maintenance requirements of the system. Instead of using the active or passive filters, a virtual impedance control methodologies have been used in literature. These have an advantage over other methodologies as they do not require any extra circuitry or bulky filters. The cost of the system also does not increases. However, using the virtual impedance control methodologies may have the effect of degradation of the dynamics

of the system if not designed properly. These filters use the capacitor or inductor as the ripple energy storing element. However, it leads to an increase in the component count. In this work, different robust virtual impedance shaping methodologies are proposed so as to mitigate the SRCs or regulate the SRCs to be within some desired limits.

These second-order oscillations occur in the voltage source inverters, current source inverters, single-stage inverters etc. The single-stage inverters are used to obtain the AC voltage greater than the input DC voltage. The impedance network at the input of the SSIs facilitates the boosting of input DC voltage. The impedance network is designed by taking the switching frequency into consideration. The higher the switching frequency, the smaller are the components required for the impedance network. The frequency of the SRCs is much less compared to the switching frequency of the SSIs. The voltage boosting depends on the shoot through duty cycle of the SSIs. The higher the shoot through duty, higher is the output AC voltage, and higher is the second-order ripple content in the source current. This SRCs propagates through the impedance network to the source and affects it. In the distributed power generation system like the DC microgrid, the second-order currents gets distributed among the sources according to the connecting cable impedance. The SRCs propagate to a node with less output impedance as seen from the DC bus.

The objective of the proposed robust impedance shaping methodology is to design the SRC regulating control algorithm without any increase in the component count or without the addition of any extra filter circuitry. The proposed control algorithms facilitate the usage of smaller capacitance, which allows usage of non-electrolytic capacitors. This has a direct impact on the reliability of the system. The proposed control techniques increase the impedance of the inductor branch of the converter virtually. As a result, the SRCs follow the low impedance path and flow to the capacitors. Further, the SRC regulating controllers must ensure minimal degradation of converter dynamics along with reducing the SRCs. In literature, various linear controller-based methodologies are available, which change the bandwidth of the control loops to regulate the SRCs. This has the direct impact of degradation of the dynamics of the system. Any uncertainty in modeling of converters or disturbance may further degrade the dynamics. Hence, it is desired to reduce the SRCs by proposing the control methodologies, which are able to operate even in uncertain conditions and can handle the uncertainties without degrading the dynamics. In DC Microgrids, the per-unit load current value is communicated to the neighboring nodes to achieve consensus in terms of load sharing. If the shared value consists of some second order ripple terms, it will result in erroneous reference generation in the DC Microgrid. This may lead to oscillations in the dc bus voltage. A distributed control must be designed so as to cancel out these oscillations and other bounded known disturbance, to ensure robust control of Microgrids. The control design process must consist of local node parameters so as to ease the design process. In terms of SRC sharing, the output impedance of a node should be regulated as per filter availability in the node, such that, if the node consists of some ripple filter, the SRC propagation to this node must be increased compared to the other nodes. This will help in increasing the ripple filter energy density. Further, the designed primary control must be easily integrated with the consensus based secondary controllers. It must be able to operate with minimal communication requirements between the neighboring nodes. Along with all the above issues, the stability of the Microgrid during the plug and play must also be ensured. Plug in and out of a node must require minimal intimation among the neighboring nodes. The load sharing must be as per the rating of the source or the interfacing converter. The voltage regulation and proportional load sharing must be maintained while regulating the SRCs within desired limits during the AC and DC load variations. To achieve robust control of SRCs, the proposed methodologies consist of sliding mode control (SMC) and integral sliding mode control (ISMCs). The SMC is known to be robust against modeling and parametric uncertainties. The surface of the SMC is designed so as to achieve the control law which results in an increase of the output impedance of converters. In

SMCs the disturbance rejection takes place once it reaches the sliding surface. To mitigate this issue, the ISMC based SRC controllers are proposed which ensure disturbance rejection from the beginning. The ISMCs are designed to cancel out the matched uncertainties which are the second order ripples in voltage and currents, and other known bounded disturbances, without amplifying the unmatched uncertainties.

1.2 CONCEPT OF IMPEDANCE SHAPING

The SRCs gets distributed as per the impedance seen from the DC bus terminals. The DC bus consists of a capacitor that has the impedance X_c as shown in Figure 1.1. The impedance reduces with the increase in the frequency. The branch consisting of the source consists of an intermediate inductor. The impedance of the inductor branch is denoted by X_L in the figure. As the impedance is proportional to the frequency term, as the frequency increases, the impedance X_L increases. Hence, at higher frequencies, the impedance of the capacitor branch is less than the inductive branch. Due to the lower impedance of the capacitor branch, the higher-order oscillations are propagated to the capacitor. However, at low frequencies, the impedance of the inductive branch is less than the capacitor branch. As a result, all the low-frequency currents propagate to the source through the inductor. The Figure 1.1 shows that the impedance X_L<X_c at 100 Hz, where 50 Hz is the AC supply frequency. To reduce these SRCs, the impedance of the inductor branch has to be increased. This can be done by increasing the inductor to increase equivalent X_L, or to increase capacitance to reduce the X_c. However, this increases the size, weight, and cost of the system. Instead, the impedance can be varied by incorporating the virtual impedance method. In this, the output impedance is varied to achieve the impedances of Z_{o1}, Z_{o2}, or Z_{o3}. It must be noticed, that the magnitude of impedances varies considerably at 100 Hz. The impedance Z_{o3}>X_c at 100 Hz.

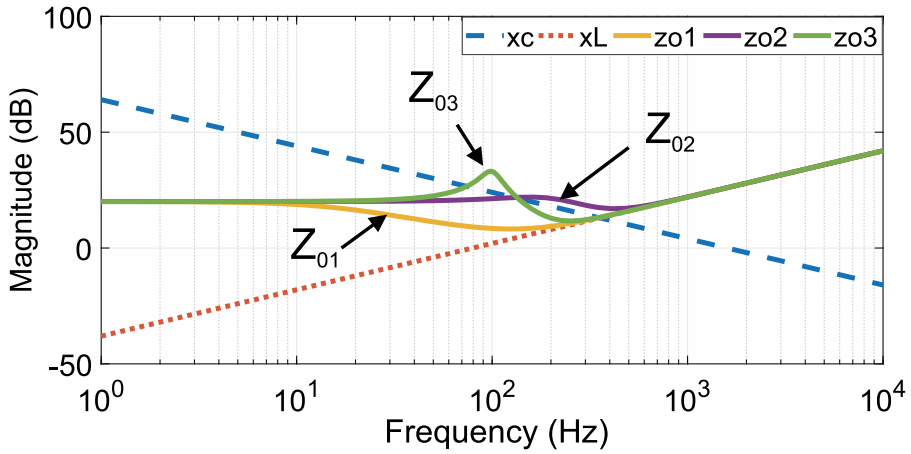

Figure 1.1 : Concept of impedance shaping

1.2.1 Virtual impedance shaping in the Single Stage Inverters

The second-order ripples are reflected on the DC side during the DC-AC conversion or vice-versa. These second-order ripples can be observed in the Voltage Source Inverters (VSIs), Current Source Inverters (CSIs). The VSIs and CSIs are widely used for industrial and household applications; however, they do not boost the input DC voltage. The output AC voltage can be regulated to be less than the input DC voltage using the modulation index. To boost the output voltage, either a step-up transformer is connected at the output terminals or an intermediate boost converter is to be incorporated. This leads to an increase in the component count of the system. Further, as the number of stages increases, the efficiency of power conversion also reduces due

to losses in the components. To address these issues, various single stage DC-AC conversion topologies have been proposed in the literature. The SSIs perform the DC-AC conversion by means of shoot through. During shoot through interval, the inverter legs are shorted, and no power is transferred to the load. This increases the rate of change of current in the input inductor. This results in the boosting of the input voltage. Hence, the output AC of a larger magnitude can be achieved without the addition of any extra components. But similar to the VSIs and CSIs, the SSIs also have second-order oscillations in the input current. In what follows, the analytical expression of the ripple power is derived.
Instantaneous output power of an inverter P_{ac} = V_{ac} I_{ac}

$$P_{ac} = V_{ac}I_{ac} = V_m cos(\omega t) I_m cos(\omega t - \phi) \tag{1.1}$$

On further expanding the above equation and dividing power into the constant DC component P_c and ripple component P_r:

$$P_{ac} = \frac{1}{2}V_m I_m cos(\phi) + \frac{1}{2}V_m I_m cos(2\omega t - \phi) = P_c + P_r \tag{1.2}$$

Where, ω is the AC supply frequency, ϕ is load power factor angle, V_m and I_m are voltage and current maximum values. As can be observed from (1.2), the ripple component of power P_r oscillates at twice the AC supply frequency (where ω is the AC supply frequency). This component is responsible for the voltage and source current oscillations.

The virtual impedance shaping for SRC mitigation in the Quasi-Z Source Inverters (qZSIs) and Embedded Quasi Switched Boost Inverter (eqSBIs) topologies of SSIs is shown in Figure 1.2 and Figure 1.3, respectively. The virtual impedance Z_v is incorporated in series with the inductor, which is closer to the source. This increases the impedance of the SSIs as seen from the inverter terminals as a result of which the SRC propagation to the source will get reduced considerably. Along with regulating the SRCs, the designed control must be able to achieve the desired voltage levels at the SSI output terminals irrespective of load variations.

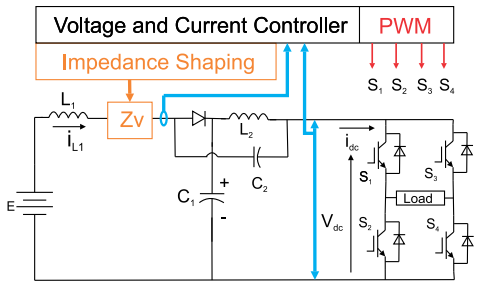

Figure 1.2 : q-Z Source Inverter

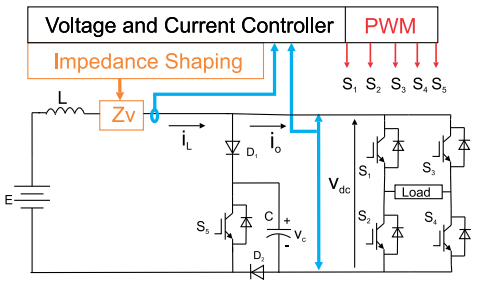

Figure 1.3 : eq-Switched Boost Inverter

Figure 1.4 : Virtual impedance shaping for SSIs

1.2.2 Virtual impedance shaping in the DC Microgrids

A DC Microgrid consists of an interconnection of sources, loads, and energy storages to a common DC bus. The interfacing converters consists of a boost converter so as to step up the source voltage to the desired DC bus voltage level. The load can be a constant resistive load, a constant power load or an inverter fed AC load. The DC load and constant power loads draw

constant power from the sources. The inverter fed load draws oscillating power from the sources. As a result of the oscillating power demand, the SRCs are reflected on the DC side. This leads to oscillations in the source currents. An analysis of SRC distribution in the microgrid is presented below:
Consider two DC-DC converters connected to a DC bus, feeding an inverter load. Let the power shared by the converters be P_1 and P_2, respectively.

$$P_1 + P_2 = P_c + P_r = \frac{1}{2}V_m I_m cos(\phi) + \frac{1}{2}V_m I_m cos(2\omega t - \phi) \tag{1.3}$$

P_c is constant DC component and P_r is the ripple component such that $P_c = V_{DC}I_c$ and $P_r = V_{DC}I_r$. Let the inverter supply a resistance load i.e. ϕ = 0, (1.3) becomes :

$$P_1 + P_2 = \frac{1}{2}V_m I_m + \frac{1}{2}V_m I_m cos(2\omega t) \tag{1.4}$$

If $\phi \neq 0$, then also the second order ripple term persists, however, for simplicity of derivation consider only a resistive load. Individual power generated by each sources is divided into following parts, constant DC part P_{c1} and P_{c2} and ripple component P_{r1} and P_{r2} respectively.

$$(P_{c1} + P_{r1}) + (P_{c2} + P_{r2}) = \frac{1}{2}V_m I_m + \frac{1}{2}V_m I_m cos(2\omega t) \tag{1.5}$$

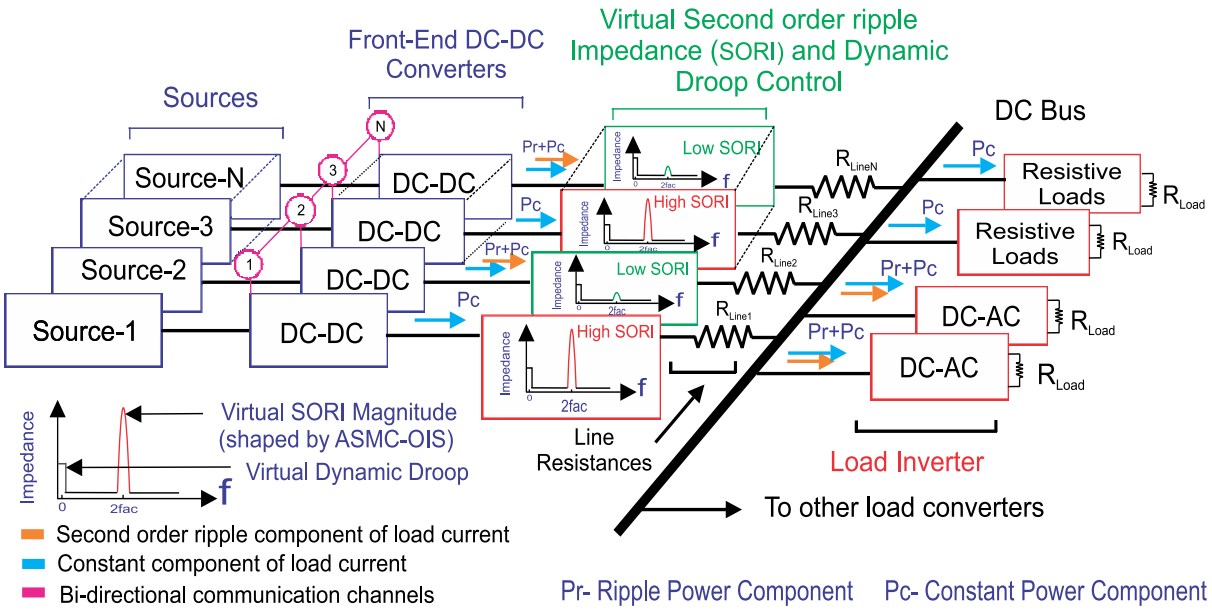

Figure 1.5 : Proposed power sharing scheme: High and low impedance at $2f_{ac}$ is achieved by output impedance shaping

By separating the constant and ripple components and substitute $V_m = V_{DC}$ and normalizing by a suitable base current value I_b so as to obtain per unit current $I_{ci}^{pu} = \frac{I_{ci}}{Ib}, I_{ri}^{pu} = \frac{I_{ri}}{Ib}, I_{mi}^{pu} = \frac{I_{mi}}{Ib}$:

$$I_{c1}^{pu} + I_{c2}^{pu} = \frac{1}{2}I_m^{pu} \tag{1.6}$$

$$I_{r1}^{pu} + I_{r2}^{pu} = \frac{1}{2}I_m^{pu} cos(2\omega t) \tag{1.7}$$

A microgrid may consist of several other nodes connected in parallel. Generalize (1.6) and (1.7) for N converters as:

$$\sum_{i=1}^{N} I_{ci}^{pu} = \frac{1}{2} I_m^{pu} \quad , \quad \sum_{i=1}^{N} I_{ri}^{pu} = \frac{1}{2} I_m^{pu} cos(2\omega t) \tag{1.8}$$

$$\frac{I_{r1}^{pu}}{I_m^{pu}} + \frac{I_{r2}^{pu}}{I_m^{pu}} + ... + \frac{I_{rn}^{pu}}{I_m^{pu}} = \frac{1}{2} cos(2\omega t)$$

Let

$$\gamma_1 = \frac{I_{r1}^{pu}}{I_m^{pu}} \qquad \gamma_2 = \frac{I_{r2}^{pu}}{I_m^{pu}} \quad ..... \qquad \gamma_n = \frac{I_{rn}^{pu}}{I_m^{pu}}$$

$$\gamma_1 + \gamma_2 + ...\gamma_n = \frac{1}{2} cos(2\omega t) \tag{1.9}$$

$$\sum_{i=1}^{N} \gamma_i = \frac{1}{2} cos(2\omega t) \tag{1.10}$$

If we control the SRC of first converter the γ_1 would tend to be 0.

$$\sum_{i=2}^{N} \gamma_i = \frac{1}{2} cos(2\omega t) \tag{1.11}$$

Hence, all γ_i's has to increase to satisfy the above equation, and ripple sharing is achieved. The virtual impedance shaping must be designed so as to have minimal effect on the dynamics of the system. The designed controller must be able to mitigate the second-order ripples in presence of uncertainties. In DC Microgrid, the SRC mitigation of distribution must be regulated along with the proportional DC load sharing.

An overview of the concept of SRC sharing is illustrated using the Figure 1.5. It shows a DC Microgrid formed by the interconnection of four nodes. Both the resistive loads, as well as the DC-AC converters, are connected to the DC bus. The figure shows the need for varying the impedance of the interfacing converter so as to regulate the SRC content at a node. The nodes with higher second-order ripple impedance (SORI) only provides the constant DC component of the power demanded from the AC load. The nodes with less SORI provide both the second-order P_r and the constant component P_c of the AC load demand. The requirements of the virtual impedance control are mentioned in the next section. An illustration of microgrid current distribution without virtual impedance control is shown in Figure 1.6, and Figure 1.7. The figure shows that in absence of any impedance control, the loads get arbitrarily shared among the interfacing converters. On the other hand, the virtual impedance Z_v and R_d can be used to regulate the SRC and proportional load distribution among the microgrid sources.

1.3 REQUIREMENTS FOR THE SRC CONTROL

The SRC control is achieved by increasing the impedance of the inductor virtually by means of control. However, various aspects must be addressed such that the designed control must operate the converter as desired. The aspects can be described as follows:

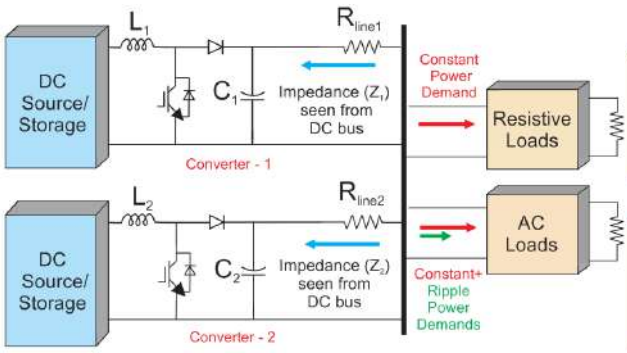

Figure 1.6 : Without impedance control

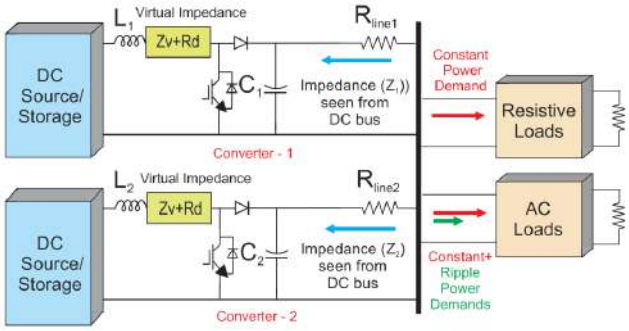

Figure 1.7 : Virtual impedance control

Figure 1.8 : A two node microgrid

1.3.1 Requirements for the SRC control in the Single Stage Inverters:

- The dynamic characteristics should not get degraded to ensure a good power quality at the output terminals.
- The SRC controller must not affect the voltage and current control loops in case of dual-loop control.
- The SRC control must be robust against various modeling and operating uncertainties.
- The SRC must be regulated for a wide range of load variations.

1.3.2 Requirements for the SRC control in the DC Microgrid system:

- The SRC control must not affect the proportional load sharing among the interfacing converters.
- It must mitigate any uncertainty in microgrid modeling or known bounded disturbances.
- The design process must use the local parameters, preferably. This eases the design process.
- It must facilitate the plug and play of various nodes while regulating the SRC content at a node.
- It must be easily integrated with the traditional hierarchical control in the DC Microgrid control.

1.4 PROPOSED CONTROL METHODOLOGIES

To achieve the above mentioned requirements of SRC control, a class of robust control methodologies have been proposed in this thesis. The proposed methodology consists of dynamic output impedance shaping based on the dual loop control, SMC based SRC control and ISMC based SRC control. In dual loop control based SRC mitigation methodology, a SRC control loop is integrated with the the inner current control to vary the output impedance as per the SRC reference of a node. For a high SRC content, the impedance is increased until the SRC drops down to the desired limit. To make the SRC control robust, SMC based SRC control is proposed for DC

Microgrid and nanogrid application. The inductor current reference is obtained by passing the instantaneous current through a low pass filter with cutoff frequency less than the second order ripple frequency. This results in an increase of impedance virtually. Further, an adaptive SMC is proposed for implementation in the primary control of DC Microgrids. The designed adaptive control requires the local parameters of the node. To facilitate the plug and play operation, a dynamic coefficient is incorporated in the sliding surface to ensure a fast convergence to the desired operating point. To further improve the performance of system in uncertain operating conditions, the ISMC is integrated with the dual loop control for SSIs. In DC Microgrid, a robust ISMC based secondary control is proposed to cancel out the SRC terms in the communicated data between the neighboring nodes. The proposed methodologies are briefly explained to ensure continuity in subsequent chapters:

1.4.1 Dual loop control integrated with the second-order ripple control loop

In this methodology, a dual loop control is integrated with a separate impedance control loop, as shown in Figure 1.9. The inner current control loop is designed to operate faster than the outer voltage control loop. The voltage controller is G_v and the current controller is G_i. The dynamics of the impedance shaping loop is designed to be in between the inner and the outer loops. The output of the impedance shaping loop varies the virtual impedance magnitude, so as to reduce the SRC content. The SRC content is extracted using the second-order general integrator(SOGI) tuned at second order ripple frequency and is given as the reference, which is then compared with the actual SRC content of the node. The error is fed to the PI controller, which adjusts the impedance value. The inductor current of the terminal in which the impedance is to be increased is fed to the control loop through an inverted notch filter G_{notch}. This control methodology does not require feedback from the load terminals. This makes it applicable to SRC mitigation in the distributed environment like the DC Microgrids.

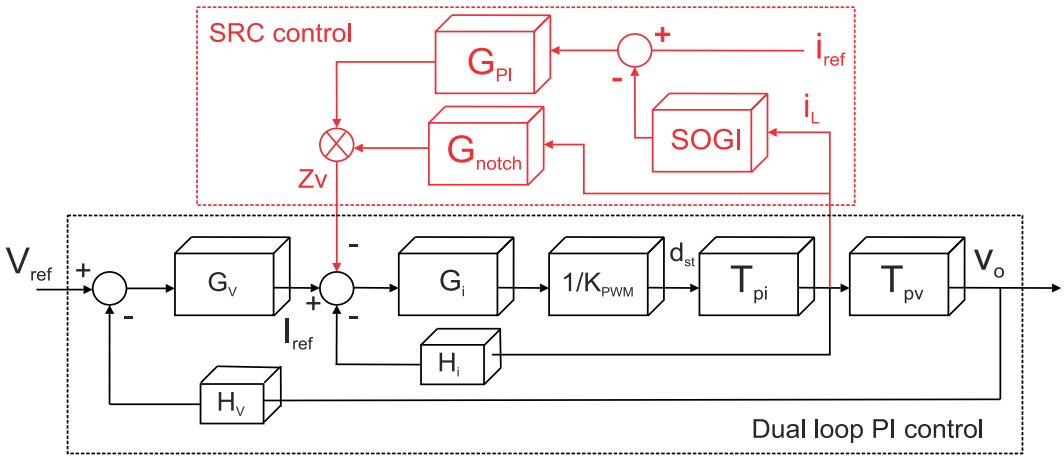

Figure 1.9 : Proposed dual loop with SRC control loop

1.4.2 Linear control integrated with ISM control

In this methodology, a robust integral sliding mode control is used so as to mitigate the SRCs along with the known bounded uncertainty. The control has been implemented in Single-Stage Inverters. The ISM Castanos and Fridman [2006]; Utkin and Jingxin Shi [1996] surface consists of the desired and actual dynamics. A non-linear control law is generated from the ISM controller. The integral sliding mode control is added with the linear control law obtained from dual-loop control so as to mitigate any effect of matched disturbances. Consider the dynamics as in (1.12), with matched $d_m(t,x)$ and and unmatched uncertainties $d_u(t,x)$ as-

$$\dot{x} = Ax + Bu + d_m(t,x) + d_u(t,x) \tag{1.12}$$

The purpose of ISMC is to mitigate $d_m(t,x)$ without amplifying $d_u(t,x)$. Let the sliding surface to be chosen as-

$$s(t) = G(x(t) + z(t)) \quad \dot{s} = G(\dot{x}(t) + \dot{z}(t)) \tag{1.13}$$

where,

$$\dot{z}(t)) = -G(Ax + Bu_l),\ z(o) = G(x(o)),\ u_n = -d_m(t,x). \tag{1.14}$$

From (1.12), substitute the value of $\dot{x}(t)$,

$$\dot{s} = G(Ax + Bu + d_m(t,x) + d_u(t,x) + \dot{z}(t)) \tag{1.15}$$

In the above equation, the control signal u is the sum of linear controller and ISM controller. Hence, substitute $u = u_l + u_n$ in above equation,

$$\dot{s} = G(Ax + B(u_l + u_n) + d_m(t,x) + d_u(t,x) + \dot{z}(t)) \tag{1.16}$$

As of now, let the unmatched uncertainty be negligible, i.e. $d_u(t,x)$=0, during sliding mode, the sliding surface reduces to,

$$\dot{s} = G(Bu_n(t) + Bd_m) \tag{1.17}$$

Hence, in case of matched uncertainty, the ISM will only cancel out the unknown disturbance, and the linear controller will control the plant without any disturbance. In case of unmatched disturbance, $d_u(t,x) \neq 0$. The control law becomes $u_n = (-d_m(t,x) - (GB)^{-1}Gd_u(t,x))$, and dynamics become,

$$\dot{s} = Ax + Bu_l + (I - B(GB)^{-1}G)d_u(t,x) \tag{1.18}$$

The value of G must be selected such that the product of GB=I, where I is the identity matrix. As a result of this, G=B^{-1}. The input matrix B is not a square matrix, as a result of this, pseudo inverse of B has to be calculated to obtain the value of G. Such inverse is also called the Moore-Penrose inverse. Hence, the value of G=B^{+}. Now, that the parameters are defined, the ISMC based control law becomes $u_n = -\rho sign(s)$. The parameter ρ must be a value which is more than the magnitude of unknown disturbance. The overall control law will be sum of linear control law and ISM based control law. The resulting control law is the shoot through duty cycle which decides the duration for which the inverter switch are to be shorted. The modulation index is obtained from the shoot through duty cycle by substracting it from unity. The control logic is shown in Figure 1.10

1.4.3 Sliding mode control methodology

The sliding mode control is a variable structure control methodology that is known to be robust against modeling uncertainties. By implementing SMC, the benefits of SRC reduction along with robust control, can be achieved. The sliding manifold consists of the voltage and current errors. The voltage error is the difference between the desired and the actual voltage at the terminals. On the other hand, the current error depends on the difference between the actual current and the current passed through a low pass filter. The cutoff frequency of the low pass filter must be designed to be less than the second-order frequency. This will generate the control signals which will drive the Single Stage Inverters to reduce the SRC content in the source currents. The SMC is a non-linear control methodology, hence the stability of the system is analyzed using Lyapunov's function. The phase plane with the constant and dynamic surface is shown in Figure 1.11.

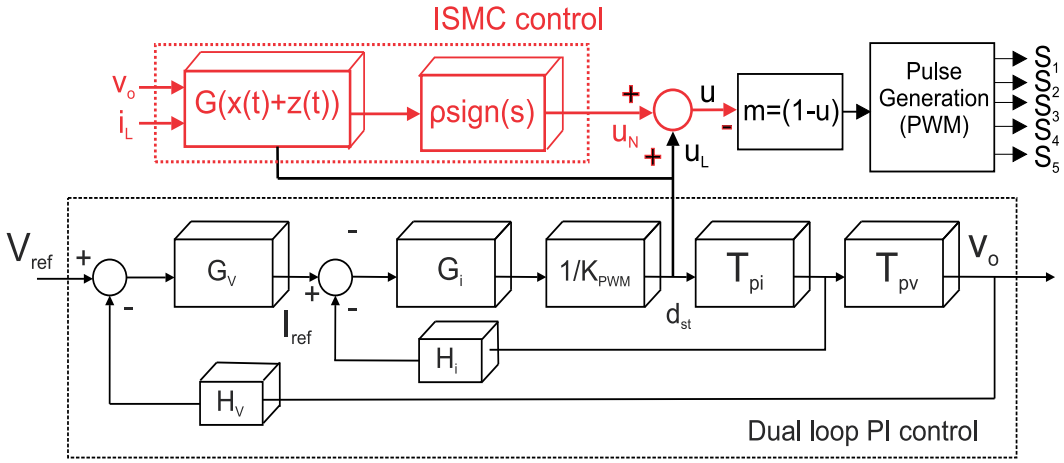

Figure 1.10 : Proposed dual loop with ISM control

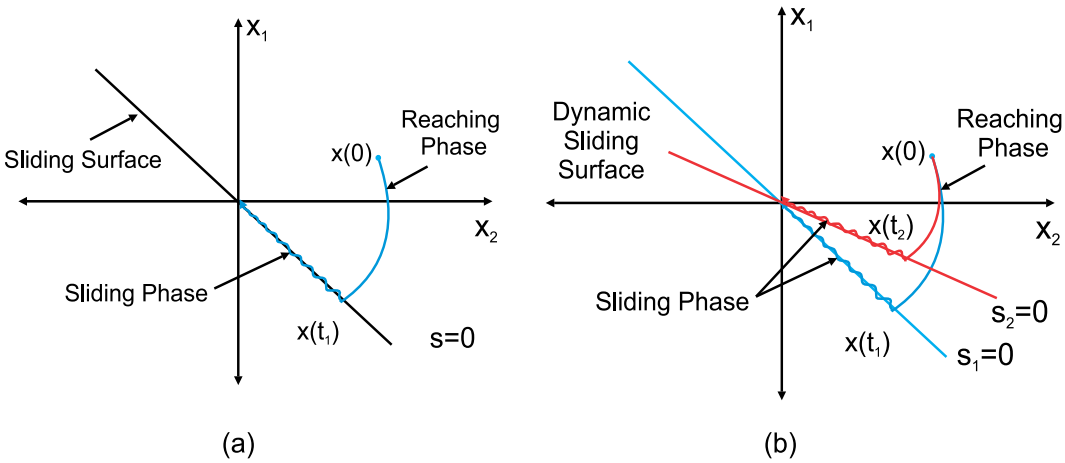

Figure 1.11 : Sliding mode control (a) Constant Surface (b) Dynamic Surface

1.4.4 Adaptive sliding mode control methodologies

The sliding manifold in an SMC consists of voltage and current error terms. The sliding surface can be made dynamic by designing a dynamic variable such that its value depends on the voltage and current error terms. When the voltage error is out of a certain bound, the surface must consist of the voltage error term, and once the voltage error converges to zero, the surface must consist of the current error terms. As a result of this, the dynamic performance of the system get improved. By using the above concept, the surface can be properly designed such that the SRC can be regulated, and the voltage is maintained within some desired voltage regulation limit. The benefit of using such a control is that the global convergence to a value can be achieved by local designing of the controllers. This makes the control more suitable in the distributed system like the DC Microgrids. The interfacing converter's control can be designed by adaptive SMC methodology, and then it can be interfaced with the secondary and tertiary controllers of the DC Microgrid. Hence, designing the controllers at each node become easy as only local parameters will be required to design the control methodology.

1.4.5 Integral Sliding Mode control based secondary control

The DC Microgrid control must be robust in nature so as to mitigate any modeling uncertainty or other bounded disturbances. The hierarchical control of a DC Microgrid consists of a primary control that receives the operating references from the secondary controller. An integral sliding mode based secondary control is proposed so as to mitigate any uncertainty in the communicated data between the nodes. The primary control consists of a dynamic sliding manifold which maintains stability during the plugin and out of nodes. The designed, robust control improves the dynamic performance of the microgrid.

1.5 PRELIMINARIES

The proposed robust virtual impedance shaping methodologies are based on the sliding mode control and integral sliding mode control. Further, the data exchange among the nodes in the DC microgrids uses results from the graph theory. For the continuity, a brief explanation of the concepts is presented below. For a detailed understanding of the concepts, reader is encouraged to use the provided references.

1.5.1 The concept of Sliding Mode and Integral Sliding Mode Control

The Sliding Mode Control is a type of non-linear control method in which the system trajectories are regulated by using a discontinuous control law. It involves designing a suitable sliding surface, which is a combination of some desired states of the system. The control law forces the trajectories to reach the surface within some finite time interval. Once the trajectories reach the surface, the sliding motion is said to occur. The design process in SMC basically consists of two parts:
1. Designing a suitable sliding surface.
2. Design of the control law to ensure existence of sliding mode.
The advantage of using the SMC is its robustness against the modeling and parametric uncertainties.

The sliding mode control can be explained by considering an example of a second-order system Utkin [1999]:

$$\ddot{x} = ax + u \tag{1.19}$$

For the above system, choose $u = -ksign(s)$, where s is the sliding surface $s = bx + \dot{x}$. The specified system shows two different structures, for control inputs $u^+(x,t)$ and $u^-(x,t)$ as shown in Figure 1.12. The Figure 1.12(a) shows the trajectories with only $u^+(x,t)$ as the control input. Similarly, the Figure 1.12(b) shows the trajectories with $u^-(x,t)$ as the control input. The control input is $u^+(x,t)$ when $s > 0$ and $u^-(x,t)$, when $s < 0$. Figure 1.12(c) shows the sliding motion of the trajectories when the sliding mode control is implemented. The time taken for the trajectories to reach the surface is known as the reaching time. The reaching time must be finite, and the trajectories must asymptotically converge to the origin after hitting the sliding surface. It must be emphasized that the variables x shown in the figure is the error term, hence the convergence to zero means that the desired state is achieved. To ensure the existence of the sliding mode, the reachability condition must be satisfied Edwards and Spurgeon [1998]. The reachability condition states that $s\dot{s} < 0$. The inherent advantage of using the sliding mode control is that it is robust against uncertainties. However, in sliding mode control, the disturbance is mitigated once the trajectories hit the surface and during the sliding motion. To eliminate this, an integral sliding mode control is proposed in Utkin and Jingxin Shi [1996]. The integral term in the sliding manifold ensures that the system trajectories start from the sliding manifold right from the beginning. As a result, the system becomes robust, and disturbances are mitigated from the stating Castanos and Fridman [2006]. The ISMC control signal is added with a nominal control signal. The nominal controller regulates the

system performance as desired, and the ISMC control mitigates the matched disturbances without amplifying the unmatched ones. The disturbances which are in the range space of the system input matrix are called the matched disturbances. All disturbances which do not lie in the range space of the input matrix is called the unmatched disturbances Lin [2007].

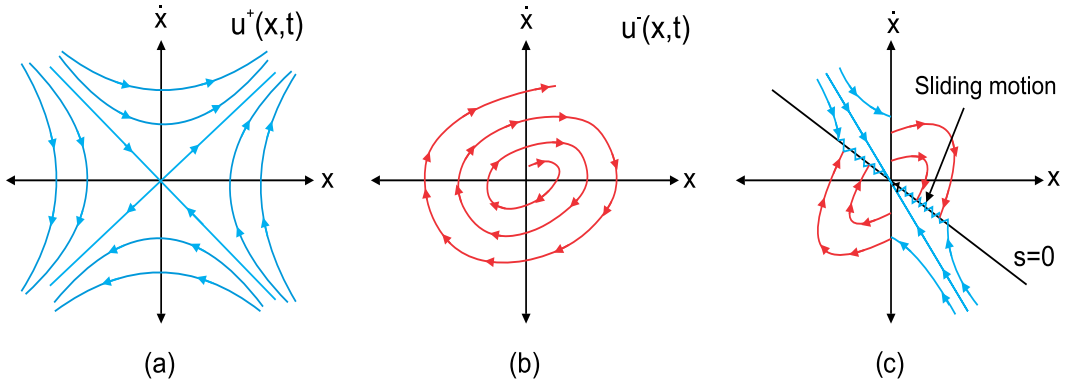

Figure 1.12 : System Dynamics: (a) With $u^{+}(x,t)$, (b) With $u^{-}(x,t)$, (c) Dynamics with sliding mode control

1.5.2 Graph Theory

A microgrid consists of various converters which are connected to a common DC bus. The distributed control of a microgrid consists of data exchange between the controllers of the converters. The communication network in a microgrid can be represented by a graph $\mathcal{G}$. The graph $\mathcal{G}$ consists of the nodes, which are the converters, and the edges represent the communication link between the nodes. The set of communication links (edges) are represented by $\mathcal{E}$. If there is exchange of data between the i^{th} and j^{th} node, then the edge e_{ij} belongs to the set $\mathcal{E}$. Similarly, the set of nodes is represented by $\mathcal{V}$. The graph of communication topology is represented by an adjacency matrix A, which consists of elements a_{ij} such that, $a_{ij} = 1$ if their data is exchanged between the nodes, else it is zero. A directed graph or digraph consists of the direction of the data transfer between the nodes. A directed graph is balanced if $\sum_{i=1}^{N} a_{ij}$=$\sum_{i=1}^{N} a_{ji}$, where N is the total number of nodes in the network. The degree matrix $\mathcal{D}$ is a diagonal matrix and consists of $\sum_{i=1}^{N} a_{ij}$. Using the adjacency matrix and degree matrix, the Laplacian $\mathcal{L}$ of the network is defined as $\mathcal{L}$=$\mathcal{D}$-$\mathcal{A}$. The row and column sum of a $\mathcal{L}$ is zero, and it is symmetric. The second smallest eigenvalues of $\mathcal{L}$ represents the algebraic connectivity of $\mathcal{G}$. The null space of $\mathcal{L}$ represents the number of connected components of the graph $\mathcal{G}$. For further insights the reader is encouraged to follow Bullo [2019]; Lewis *et al.* [2014].

1.6 CONTRIBUTIONS

The contributions of the research are briefly described as follows:

The first work consists of SRC mitigation in the single-stage inverter. A sliding mode control based methodology is proposed to regulate the output AC voltage within the desired limits and regulate the SRC simultaneously. The inductor current reference is obtained by passing it through a low pass filter. The control logic using- And, Or gates is presented. The SRC control for qZSI and EqSBI has been presented. The simulation and experimental results verify that the ripple gets reduced from 2A to 0.7A in qZSI and from 2A to 0.2A in EqSBI. To further improve the performance in the presence of the matched and unmatched uncertainties, an integral sliding mode control loop is integrated with a dual-loop voltage and current control loop in the next work.

The second work proposes a SRC mitigation control which consists of an integration of the dual-loop control and the ISMC. The dual-loop control acts as a nominal control and is responsible for maintaining the desired AC voltage at the output terminals, and the ISM is responsible for generating the non-linear control laws so as to cancel out the SRC components of the voltage and current. The proposed control mitigates the SRCs by increasing the inductance virtually, even in the presence of uncertainties. The SRC is mitigated without any degradation in the dynamics of the dual-loop control. The proposed methodology has been verified for two SSI topologies-quasi-Z Source inverters (qZSIs) and embedded quasi-Switched Boost Inverters (eqSBIs). These two topologies have been chosen as their operation is similar to a wide range of other SSI topologies. The proposed control mitigates the ripples in the source current irrespective of load changes and uncertainties in both the SSIs. In the next work, the robust virtual impedance methods have been proposed for a DC Microgrid system.

The third work proposes a distributed control strategy to regulate the current ripples propagating to the sources, in a DC Microgrid feeding both the AC and DC loads. The proposed control methodology regulates the output impedance of the source interfacing DC-DC converter dynamically at twice the AC supply frequency. The impedance is increased virtually in series with the inductor of the DC-DC converter by a dedicated controller, which regulates the ripple magnitude according to the harmonic reference. Using this, the second-order ripple currents can be mitigated or propagated to the nodes having some ripple absorbing circuits, or filters. This improves energy density in ripple filters installed at a node. The proposed control ensures ripple mitigation irrespective of the DC or AC load variations. Further, the effectiveness of proposed control is analyzed in the presence of communication delays between the nodes. A low bandwidth communication is incorporated so as to facilitate the per-unit current exchange between the nodes for the proportional DC load sharing. The reference generated by the secondary control layer may consist of oscillations due to the second-order ripples. These oscillations must be mitigated for desirable control of DC bus voltage; else it may result in oscillations. The next work consists of a robust ISMC based secondary control, which provides the reference to a sliding mode control based primary control.

The fourth work proposes an integral sliding mode control (ISMC) based secondary controller, which tunes the voltage reference within regulation range and also mitigates the bounded uncertainties in the communicated microgrid load data. This facilitates proportional load sharing even in uncertain conditions. The proposed secondary control compares the actual node parameters with the desired global reference values and generates the control signal, which is added with the primary controller's control signals. The proposed control methodology requires only local parameters for formulation. This eases the control design process. Further, a sliding mode control based primary control (SMPC) is proposed to regulate the voltage of a node and facilitate proportional load sharing among the interfacing converters. The proposed robust SMPC has excellent control during load transients and plug-in and out of nodes from the DC bus. The

primary control must be made robust such that it can be integrated with the consensus-based secondary control layer. The next work consist of an adaptive sliding mode control based primary control to regulate the SRC propagation the a node.

The fifth work consists of an adaptive sliding mode control based output impedance shaping (ASMC-OIS) methodology is proposed for voltage regulation, proportional load sharing, and second-order ripple management in a DC Microgrid. By using the proposed control method, the magnitude of the output impedance of the source interfacing converter is increased at twice the supply AC frequency programmable, which results in the reduction of second-order ripple currents propagating through the converter. Instead, it is propagated to the DC-link capacitor or towards the nodes, which consists of some ripple absorption active or passive filter. This leads to an increase in the energy density of the ripple filters. The dynamic consensus-based secondary control is incorporated to ensure proportional load current sharing. A graph theoretical analysis is presented to analyze per unit load sharing among all the nodes. The stability of the proposed controller is analyzed considering multiple source nodes using Lyapunov's approach. A DC Microgrid consisting of parallel-connected DC-DC boost converters, DC load, and inverter load is simulated to verify the proposed control strategy.

1.7 ORGANIZATION OF THESIS

The thesis is organized in eight Chapters, and the content of each chapter is briefly discussed here,

Chapter First: In this chapter, an introduction to the second-order harmonics in SSIs and DC Microgrid is presented. The chapter gives a brief description of the robust methodologies proposed. The chapter presents the main objective, motivation, and organization of the Thesis.

Chapter Second: This chapter consists of a brief literature review of various methodologies adopted for SRC mitigation. Various active, passive, and control based SRC reduction methodologies are discussed.

Chapter Third: In this chapter a sliding mode control based SRC reduction methodology for q-ZSI and eq-SBI is presented. The small-signal modeling of the SSIs is derived so as to obtain the desired control law. Further, the bounds on the low pass filter time constant are derived so as to maintain stability while reducing the SRC content in the source current. The simulation and experimental results have been presented so as to verify the proposed control strategy.

Chapter Fourth: In this chapter, a dual loop control is integrated with a non-linear ISM based control is presented. This control results in SRC reduction along with bounded uncertainty mitigation. The control methodology is designed for both the q-ZSI and eq-SBIs. The non-linear control law is derived with the desired boundary conditions for the existence of the sliding mode. The performance of control with a wide range of load variations is presented in the chapter.

Chapter Fifth: This chapter consists of SRC regulation in the distributed power generation environment like DC Microgrid. Dual loop control is used to regulate the SRC, and a separate loop is designed, which varies the virtual impedance in series with the inductor. The SRC reference to a node is provided, and accordingly, the virtual impedance is shaped. As a comparison, the impact on the system dynamics by increasing the passive components and by using the virtual impedance methodology is presented. The simulation and experimental results are presented to verify the impedance variation at the desired node of the microgrid.

Chapter Sixth: In this chapter, a dynamic surface sliding mode control is integrated with an ISM based secondary controller. The dynamic SMC results in a good voltage regulation during the plug and play control. The secondary ISM based control mitigates the uncertainties in the voltage reference provided to the primary control. The derivation of the primary control law is presented. The secondary control designing is also discussed in the chapter. The simulation and experimental results show that the uncertainty is mitigated successfully and the proportional

sharing is maintained during the plug and play of either a highly loaded or a less loaded node.
Chapter Seventh:. Finally, a dynamic sliding manifold is presented in this chapter. The proposed control is capable of regulating the DC bus voltage and SRC content of the node simultaneously. The bounds of control parameters are derived. The stability of the control is evaluated using the Lyapunov's function. The negative definiteness of the Lyapunov's function ensures the asymptotic stability of the system. The control is applicable to the DC Microgrid. The impedance variation at some desired frequency is analyzed by frequency sweep. The control performance is evaluated for a wide range of AC and DC load variations.

Chapter Eighth: Presents the discussion and conclusion of the thesis. Various open problems that can be addressed have also been discussed.

1.8 PUBLICATIONS

1. S. Chaturvedi, D. Fulwani and J. M. Guerrero, "Adaptive-Sliding-Mode-Control based Output Impedance Shaping for Ripple Management in DC Microgrids Affected by Inverter Loads," in IEEE Transactions on Sustainable Energy. (Published)

2. S. Chaturvedi, D. Fulwani and D. Patel, "Second Order Ripple Mitigation in DC Microgrids affected by Inverter Loads,"-in IEEE Transactions on Power Electronics (Published).

3. S. Chaturvedi, D. M. Fulwani and D. Patel, "Dynamic Virtual Impedance based Second Order Ripple Regulation in DC Microgrids", Journal of Emerging and Selected Topics in Power Electronics. (Review Submitted)

4. S. Chaturvedi, D. Fulwani, "A Double Line Frequency Ripple Control using Integral Slid- ing Mode for qZSI and eqSBI,"-in IEEE Transactions on Power Electronics (To be submitted).

5. S. Chaturvedi and D. M. Fulwani, "Adaptive Voltage Tuning Based Load Sharing in DC Microgrid," 2019 IEEE Industry Applications Society Annual Meeting, Baltimore, MD, USA, 2019, pp. 1-6.

6. S. Chaturvedi and D. M. Fulwani, "Adaptive Voltage Tuning Based Load Sharing in DC Microgrid," 2020 IEEE Transactions on Industry Applications.

7. Chaturvedi S., Fulwani D.M.,"Control of Single Stage Inverters and Second Order Ripple Regulation Using Sliding Mode Control"- Emerging Trends In Sliding Mode Control-Theory and Application.

8. S. Chaturvedi and D. M. Fulwani, "Second Order Ripple Reduction in Switched Boost Inverter For Standalone Nanogrid Applications," 2019 IEEE 4th International Future Energy Electronics Conference (IFEEC), Singapore, Singapore, 2019, pp. 1-6.

9. S. Chaturvedi and D. Fulwani, "Integral Sliding Mode Control for Uncertainty Mitigation in Switched Boost Inverters," 2020 IEEE 9th Power India International Conference (PIICON), SONEPAT, India, 2020, pp. 1-6, doi: 10.1109/PIICON49524.2020.9112872.

10. S. Chaturvedi and D. M. Fulwani, "Virtual Impedance based Second Order Ripple Control For Non-Inverting Buck-boost Converter," 2020 IEEE Industry Applications Society Annual Meeting, Detroit, MI, USA.

11. Chaturvedi S., Fulwani D.M. (2020) Equal Load Sharing in DC Microgrid Using Line Resistance Estimation. In: Mehta A., Rawat A., Chauhan P. (eds) Advances in Control Systems and its Infrastructure. Lecture Notes in Electrical Engineering, vol 604. Springer, Singapore